Application of a Probabilistic Method Based on Neutrosophic Number in Rock Slope Stability Assessment

Article *in* Applied Sciences · June 2019

DOI: 10.3390/app9112309

CITATIONS
0

READS
9

4 authors, including:

Jun Ye
Shaoxing University
200 PUBLICATIONS **5,371** CITATIONS

SEE PROFILE

applied sciences

MDPI

Article

Application of a Probabilistic Method Based on Neutrosophic Number in Rock Slope Stability Assessment

Bo Li [1], Kaifeng Zhou [1], Jun Ye [2] and Peng Sha [1,*]

[1] Key Laboratory of Rock Mechanics and Geohazards of Zhejiang Province, Shaoxing University, 508 Huancheng West Road, Shaoxing 312000, China; libo@usx.edu.cn (B.L.); zkfhsa@163.com (K.Z.)

[2] Department of Electrical and Information Engineering, Shaoxing University, 508 Huancheng West Road, Shaoxing 312000, China; yejun@usx.edu.cn

* Correspondence: shapeng@usx.edu.cn; Tel.: +86-575-88346557

Received: 8 April 2019; Accepted: 30 May 2019; Published: 5 June 2019

Featured Application: A vector similarity measure under neutrosophic number environment was developed for rock slope stability assessments with multiple levels of attributes. This method does not require sophisticated modeling of slopes and the data demand is relatively low. It could serve as a quick preliminary method to identify the key influential parameters and the risk of natural hazards, such as rock slope failures.

Abstract: The stability of natural rock slopes is influenced by a wide spectrum of factors, such as mechanical properties of bedrocks and spatial distribution of discontinuities. Their specific values are typically incomplete, due mainly to the lack of effective and comprehensive methods to accurately characterize these factors, especially those inside of the slopes. The neutrosophic number is a useful tool to solve problems in indeterminate environment. This study introduces the neutrosophic theory into slope stability assessment. A vector similarity measure developed under neutrosophic environment was employed to establish a stability assessment method considering multilevel attributes of slopes. Using this method, the level of stability for studied slopes, i.e., stable, mostly stable, less stable, and instable, was determined by computing the relation indices. The method was applied to a group of rock slopes located in Zhejiang province, China, and the calculated results were compared with the reality of in situ survey. The field application showed that the developed method has a good efficiency and precision in assessing the stability of rock slopes. The obtained weight vector can reveal the key influential parameters that inherently control the stability of rock slopes.

Keywords: rock slope stability assessment; probabilistic method; neutrosophic number; vector similarity measure; multiattribute classification

1. Introduction

Rock slope failures are a typical type of geological hazard that feature large scale and serious damage, frequently occurring in mountainous regions. Rock slopes can be considered as a complex system that consists in random, discrete, and nonlinear information, such as the characteristics of geological structures, geomorphic types, and environmental impacts [1–3]. For the better protection of civil engineering, environmental conservation, and efficient operation, the assessment of rock slope stability has always been a challenging topic in the world.

In the past several decades, different approaches have been developed to assess the stability of rock slopes, which can be primarily categorized into deterministic and probabilistic methods. Limit equilibrium and numerical analysis are the most common forms of deterministic method. The limit

equilibrium method utilizes the static equilibrium principle to analyze the stress state under various failure modes of slopes [4], including Bishop's, Janbu's, Morgenstern–Price's and Fellenius' techniques, etc. [5–7]. Meanwhile, different numerical methods, such as finite element method, discrete element method, discontinuous deformation analysis, and numerical manifold method, have been employed in slope stability assessments and landslide evolution, which have achieved great success [8–12]. In engineering practices, the amount of available data for analysis is commonly limited. It has been realized that the deterministic approaches frequently fail to give reliable assessment when complex slope systems are encountered [13,14], owing to the inadequacy of information regarding site characteristics as well as the inherent variability and measurement errors in geological and geotechnical parameters [15].

With the need to consider the risk and consequence of slope instability and parameter uncertainty, probabilistic approaches have been developed and applied to slope stability assessment. Different mathematics methods have been employed for rock slope engineering, such as the reliability theory, the fuzzy mathematics, the grey theory, and the artificial neural network (ANN). Early studies developed assessment models directly based on a single probabilistic method [16–20]. It has been realized later that the combination of different probabilistic methods can yield better assessments, such as the hybrid model of the projection pursuit (PP), particle swarm optimization (PSO), and the logistic curve function (LCF) [21]. The probabilistic methods have also been introduced into different failure criterions and verified against physical models to overcome the limitation of conventional methods without considering randomness and uncertainty of the slope status and mechanical parameters [22–28]. With the effort for probabilistic sensitivity analysis, more sophisticated models led to improved accuracy of assessment [29]; however, huge challenges remain in the high computational effort, complex modeling procedures, and the large amount of data required to yield results with acceptable accuracy.

In recent years, the neutrosophic theory, as a new theory of uncertainty, has been accepted and rapidly applied to different fields, such as electrical engineering, medical diagnosis, and roughness estimation [30–32]. Neutrosophic number (NN) is a branch of neutrosophy that evolved from classic philosophy. Smarandache [33–35] originally proposed the concept of neutrosophic number, which consists of both indeterminate and determinate information for a problem with uncertainty. Ye [36,37] developed three vector similarity measures, i.e., Jaccard, Dice, and cosine similarity measures, and incorporated them into the neutrosophic number to solve problems related to decision-making. Ye [38] later combined possibility degree ranking method and ordered weighted aggregation operators of interval neutrosophic numbers to handle decision-making problems. More recently, several extensions of neutrosophic theory have been put forward to deal with different types of problems. Roy and Das [39] solved multicriteria production planning problem by linear programming approaches. Abdel-Baseet et al. [40] proposed a new approach of big data analysis by neutrosophic mining algorithm, which increased the number of generated association rules. The neutrosophic number provides a simple and reliable way for assessment of uncertainty in the real world, such as probability analysis of various failure phenomena.

Extensive and detailed geological survey on slopes is essential to establish an effective regional plan for risk assessment and management of slope disasters, which, however, is not always practical in many mountainous regions, where only the geological data of a few selected slopes typically with greater risks are available. Given that most probabilistic methods require a sufficient amount of data to construct a baseline or a rule for stability assessment, the insufficiency of geological data has been a significant obstacle faced by researchers in the applications of probabilistic methods. In the present study, a new probabilistic methodology of rock slope stability assessment is developed based on the theory of neutrosophic number, aiming to provide a fast and reliable approach to assess the rock slope stability with limited geological data.

2. Materials and Methods

2.1. General Concept of Neutrosophic Number

Some scientific problems with uncertainty cannot be directly estimated in a quantitative manner in the real world. The uncertain parts need to be translated into mathematical forms for utilization. Hence, Smarandache [33] originally proposed a concept of NN to express real information. In reality, different kinds of data are used to denote different attributes, which are distinct and can be expressed by crisp numbers, such as 0 and 1. Under neutrosophic environment, the crisp number can be denoted as $N = Q + EI$, and this expression contains two parts, i.e., the determinate part Q and the indeterminate part EI, where the values Q and E represent the real number. The indeterminacy I is a dynamic interval number owing to the domain, which is variable according to the actual situation. The indeterminacy I has the following properties: $I^2 = I$, $0 \times I = 0$, and I/I = undefined.

Taking a neutrosophic number $N = 6 + 4I$, as an example, if $I \in [0,\ 0.5]$, it is equivalent to $N \in [6, 8]$ and therefore $N \geq 6$. This number consists of the determinate part 6 and the indeterminate part $4I$. The domain $I \in \left[I^L,\ I^U\right]$ can be selected according to the practical situation. Here, L and U stand for the lower and upper bounds for the domain, respectively. When an event is considered to be true, the value of indeterminacy becomes 0. For example, if the value of a true event equals to 8, the neutrosophic number will be $N \in [8,\ 8]$, and it is defined as $N = 8 + 0 \times I$.

Considering two neutrosophic numbers $N_1 = E_1 I + Q_1$, and $N_2 = E_2 I + Q_2$, where $I \in \left[I^L,\ I^U\right]$, the algorithm of neutrosophic number is as follows [27–29].

$$N_1 + N_2 = Q_1 + Q_2 + (E_1 + E_2)\, I \tag{1}$$

$$N_1 - N_2 = Q_1 - Q_2 + (E_1 - E_2)\, I \tag{2}$$

$$N_1 \times N_2 = Q_1 Q_2 + (Q_1 E_2 + E_1 Q_2 + E_1 E_2)\, I \tag{3}$$

$$N_1{}^2 = (Q_1 + E_1 I)^2 = Q_1{}^2 + \left(2 Q_1 E_1 + E_1{}^2\right) I \tag{4}$$

$$\frac{N_1}{N_2} = \frac{Q_1 + E_1 I}{Q_2 + E_2 I} = \frac{Q_1}{Q_2} + \frac{Q_2 E_1 + Q_1 E_2}{Q_2\,(Q_2 + E_2)}\, I \text{ for } Q_2 \neq 0 \text{ and } Q_2 \neq E_2 \tag{5}$$

$$\sqrt{N_1} = \sqrt{Q_1 + E_1 I} = \begin{cases} \sqrt{Q_1} - \left(\sqrt{Q_1} + \sqrt{Q_1 + E_1}\right) I \\ \sqrt{Q_1} - \left(\sqrt{Q_1} - \sqrt{Q_1 + E_1}\right) I \\ -\sqrt{Q_1} + \left(\sqrt{Q_1} + \sqrt{Q_1 + E_1}\right) I \\ -\sqrt{Q_1} + \left(\sqrt{Q_1} - \sqrt{Q_1 + E_1}\right) I \end{cases} \tag{6}$$

2.2. Development of a Multiattribute Similarity Measure

The Dice similarity measure is a kind of similarity evaluation method that is used to calculate the similarity degree between two objectives [41]. In regard to statistics, this similarity degree indicates the amount of association between two given objectives compared to the amount of association between them expected by chance [42]. Compared with other similarity measures, it can evaluate the similarity when one vector is equal to zero and its calculation process is relatively convenient. Here, the Dice similarity measure was incorporated into the neutrosophic number to develop a method for slope stability assessment, since slope is a complex system that consists of a series of variables with different ranges.

Considering two vectors $A = (a_1, a_2, \cdots, a_n)$ and $B = (b_1, b_2, \cdots, b_n)$ that feature length n and positive coordinates. The Dice similarity measure can be defined as

$$D(A, B) = \frac{2A \times B}{\|A\|_2^2 + \|B\|_2^2} = \frac{2\sum_{i=1}^{n} a_i b_i}{\sum_i^n a_i^2 + \sum_i^n b_i^2} \tag{7}$$

Presume that there are two neutrosophic numbers $N_{Aj} = a_{Aj} + b_{Aj}I$ and $N_{Bj} = a_{Bj} + b_{Bj}I$. For convenience, those numbers can be written as two sets $A = \{N_{A1}, N_{A2}, \cdots, N_{An}\}$ and $B = \{N_{B1}, N_{B2}, \cdots, N_{Bn}\}$. Then, the neutrosophic Dice similarity measure is defined as

$$D(A,B) = \frac{1}{n}\sum_{j=1}^{n} \frac{2\left[\left(a_{Aj}+\inf\left(b_{Aj}I\right)\right)\times\left(a_{Bj}+\inf\left(b_{Bj}I\right)\right)+\left(a_{Aj}+\sup\left(b_{Aj}I\right)\right)\times\left(a_{Bj}+\sup\left(b_{Bj}I\right)\right)\right]}{\left[\left(a_{Aj}+\inf\left(b_{Aj}I\right)\right)^2+\left(a_{Bj}+\inf\left(b_{Bj}I\right)\right)^2\right]+\left[\left(a_{Aj}+\sup\left(b_{Aj}I\right)\right)^2+\left(a_{Bj}+\sup\left(b_{Bj}I\right)\right)^2\right]} \quad (8)$$

Obviously, a single value can be denoted as a special interval between the lower and upper bounds. For example, a single value 6 can be transformed into an interval value [6, 6] that is computable in Equation (8). This measure $D(A, B)$ has the following properties.

$$1 \geq D(A,B) \geq 0) \quad (9)$$

$$D(A,B) = D(B,A) \quad (10)$$

$$D(A,B) = 1, \text{ if } A = B \quad (11)$$

The measure with a single attribute does not satisfy the requirement of slope stability assessment because a slope possesses attributes of various types and levels. Multiple attribute method has to be put forward to solve this problem.

The neutrosophic numbers N_{Aj} and N_{Bj} were further divided into N_{Ajk} and N_{Bjk}, which restructured the evaluation system to two levels. By doing so, both attribute and subattributes of slopes can be considered in the developed method. Let $N_{An} = \left\{N_{Aj1}, N_{Aj2}, \cdots, N_{Ajr}\right\}$ and $N_{Bn} = \left\{N_{Bj1}, N_{Bj2}, \cdots, N_{Bjr}\right\}$ be two sets of subattributes that can be expressed as $N_{Ajk} = a_{Ajk} + b_{Ajk}I$ and $N_{Bjk} = a_{Bjk} + b_{Bjk}I$. Then, the weight of elements N_{Aj} and N_{Bj} are given as $w_j \in [0,1]$ with $\sum_{j=1}^{n} w_j = 1$. The weight of subelements is evaluated as $\sum_{k=1}^{r} w_k = 1.$ and $w_k \in [0,1]$. Hence, the neutrosophic Dice similarity measure of multiple elements is denoted as

$$D_W(A,\ B) = \sum_{j=1}^{n} w_j \sum_{k=1}^{r} w_k \frac{2\left[\left(a_{Ajk}+inf\left(b_{AjkI}\right)\right)\times\left(a_{Bjk}+\inf\left(b_{BjkI}\right)\right)+\left(a_{Ajk}+sup\left(b_{AjkI}\right)\right)\times\left(a_{Bjk}+\sup\left(b_{BjkI}\right)\right)\right]}{\left[\left(a_{Ajk}+inf\left(b_{AjkI}\right)\right)^2+\left(a_{Bjk}+inf\left(b_{BjkI}\right)\right)^2\right]+\left[\left(a_{Ajk}+sup\left(b_{AjkI}\right)\right)^2+\left(a_{Bjk}+sup\left(b_{BjkI}\right)\right)^2\right]} \quad (12)$$

D_W (*A*,*B*) also satisfies the properties denoted in Equations (9)–(11).

2.3. Classification of Slope Properties

Before applying the developed method, it is required to classify the data of slopes to fit the algorithm. First, slope stability was classified into four grades: Stable (I), mostly stable (II), less stable (III), and instable (IV), which is commonly employed in previous studies and is recommended by related technical codes [43]. Then, according to the geological survey results, as presented in the next section, a set of predominant influencing factors was selected for stability classification analysis. The multiattribute classification method was adopted, which classified the property of slopes into three attributes and each attribute consisted of three subattributes. The slope classification is described as follows.

1. $H = \{h_1, h_2, h_3\}$, $h_1 = \{h_{11}, h_{12}, h_{13}\}$, $h_2 = \{h_{21}, h_{22}, h_{23}\}$, $h_3 = \{h_{31}, h_{32}, h_{33}\}$.

2. The three attributes (h_1, h_2, h_3) represents rock mass characteristics, topographic features, and hydrometeorology, respectively.

3. The nine subattributes (h_{11}, h_{12}, h_{13}, h_{21}, h_{22}, h_{23}, h_{31}, h_{32}, h_{33}) represent lithological association, slope structure, weathering degree, mean inclination, slope height, plant cover ratio, mean annual precipitation, human activity, and earthquake, respectively. Table 1 tabulates their classification results.

Table 1. Classification of attributes of slopes.

Attribute	Subattribute	Grade of Stability			
		Stable (I)	**Mostly Stable (II)**	**Less Stable (III)**	**Instable (IV)**
Rock mass characteristics	Lithological association	Hard and intact rock (<3)	Less hard and less intact rock (3–6)	Less soft and less fractured rock (6–8)	Soft and fractured rock (8–10)
	Slope structure	Homogenized Structure (<3)	Blocky structure (3–6)	Bedding structure (6–8)	Fractured and Loose structure (8–10)
	Weathering degree	Unweathered (<3)	Slightly weathered (3–6)	Highly weathered (6–8)	Completed weathered (8–10)
Topographic features	Mean inclination	<10°	10–30°	30–60°	>60°
	Slope height	<20m	20–50 m	50–100 m	100–150 m
	Plant cover ratio	High (>60%)	Moderate (30–60%)	Low (10–30%)	Bare (<10%)
Hydrometeorology	Mean annual precipitation	<500 mm	500–1000 mm	1000–1500 mm	>1500 mm
	Human activity	Very weak (<3)	Weak (3–6)	Strong (6–8)	Very strong (8–10)
	Seismic intensity	0–3	3–7	7–8	8–12

In Table 1, the subattributes have corresponding units, such as degree and meter, because these values were directly extracted from the in situ survey data. These real values are not suitable for a mathematical computation. They were thereafter transformed to normalized values by dividing each value by the maximum in each index. The normalized values are tabulated in Table 2. Note that each subattribute has slightly different intervals because the original data have different ranges, units, and characters. Variable intervals were therefore defined to accommodate their characters [44].

Table 2. Normalized value of subattributes of slopes.

H	h	I	II	III	IV
h_1	h_{11}	[0, 0.3]	[0.3, 0.6]	[0.6, 0.8]	[0.8, 1]
	h_{12}	[0, 0.3]	[0.3, 0.6]	[0.6, 0.8]	[0.8, 1]
	h_{13}	[0, 0.3]	[0.3, 0.6]	[0.6, 0.8]	[0.8, 1]
h_2	h_{21}	[0, 0.11]	[0.11, 0.33]	[0.33, 0.67]	[0.67, 1]
	h_{22}	[0, 0.13]	[0.13, 0.33]	[0.33, 0.67]	[0.67, 1]
	h_{23}	[0, 0.3]	[0.3, 0.6]	[0.6, 0.8]	[0.8, 1]
h_3	h_{31}	[0, 0.25]	[0.25, 0.5]	[0.5, 0.75]	[0.75, 1]
	h_{32}	[0, 0.3]	[0.3, 0.6]	[0.6, 0.8]	[0.8, 1]
	h_{33}	[0, 0.25]	[0.25, 0.58]	[0.58, 0.67]	[0.67, 1]

In the next step, the range for each subattribute was transformed into neutrosophic number to indicate its incomplete and indeterminate information, as tabulated in Table 3. The indeterminacy is set to $I \in [0, 0.24]$. Here, the range of I could be assigned by any value between 0 and 1 without changing the assessment results.

Table 3. Subattributes of slopes expressed as neutrosophic number.

H	*h*	I	II	III	IV
h_1	h_{11}	$0 + 1.25I$	$0.3 + 1.25I$	$0.6 + 0.8333I$	$0.8 + 0.8333I$
	h_{12}	$0 + 1.25I$	$0.3 + 1.25I$	$0.6 + 0.8333I$	$0.8 + 0.8333I$
	h_{13}	$0 + 1.25I$	$0.3 + 1.25I$	$0.6 + 0.8333I$	$0.8 + 0.8333I$
h_2	h_{21}	$0 + 0.4583I$	$0.11 + 0.9167I$	$0.33 + 1.4167I$	$0.67 + 1.375I$
	h_{22}	$0 + 0.5417I$	$0.13 + 0.8333I$	$0.33 + 1.4167I$	$0.67 + 1.375I$
	h_{23}	$0 + 1.25I$	$0.3 + 1.25I$	$0.6 + 0.8333I$	$0.8 + 0.8333I$
h_3	h_{31}	$0 + 1.0417I$	$0.25 + 1.0417I$	$0.5 + 1.0417I$	$0.75 + 1.0417I$
	h_{32}	$0 + 1.25I$	$0.3 + 1.25I$	$0.6 + 0.8333I$	$0.8 + 0.8333I$
	h_{33}	$0 + 1.0417I$	$0.25 + 1.375I$	$0.58 + 0.375I$	$0.67 + 1.375I$

When applying the neutrosophic Dice similarity measure to the collected data, the weight for each attribute and subattribute should be assigned as shown in Equation (12). The appropriate value of weight depends on the characteristics of all collected data and may be determined in a trial-and-error manner. To investigate the influence of weight on the assessment performance, all collected slopes were randomly divided into two groups (A and B), ten for each one. Group A was used to determine the weight vector and group B was used to validate the performance of the developed method. We selected three samples, five samples, six samples, eight samples, and ten samples from group A to calculate a set of weight vectors, respectively. These weight vectors were employed to assess the stability of slopes in group B. Because slopes in group B did not participate in the determination of weight, such a procedure could effectively appraise whether reasonable weight vectors exist in the developed method. The minimum sample number required to calculate a reasonable set of weight vectors can be determined.

2.4. Classification of Slope Mass Rating

To improve the understanding on the inherent correlation between the geological features of the slope with the stability, the following slope mass rating (SMR) is used to quantitatively estimate the stability of the slope [45–47].

$$CSMR = \xi RMR - \lambda F_1 F_2 F_3 + F_4 \tag{13}$$

$$\xi = 0.57 + \frac{34.4}{H} \tag{14}$$

where *CSMR* is the classification of slope mass rating, *RMR* (rock mass rating) is an empirical classification system for rock masses developed by Bieniawski [48]; F_1–F_4 are the coefficients of correction for the dip direction and dip angle of joint sets for different rock mass type λ, the attitude correlation between slope and the controlling joint sets, and the excavation method, respectively; ξ is the altitude correction factor according to the height of slope H. After *CSMR* estimation, the defined classes can be linked to the instability level of the slope as tabulated by Romana [45], where a total of 100 points were divided into equally spaced four levels (I–IV), indicating different degrees of stability.

3. Geological Background of Studied Rock Slopes

3.1. Geological Setting

The study area is located in Zhejiang province, the southeastern coastal region of China with a continental area of 101,800 km^2. As shown in Figure 1, the hilly and mountainous terrain with elevation above 300 m accounts for 70.6% of its total area. The altitude decreases gradually from the southwest to the northeast and drops in a step form. The southwest part is a mountainous region with the existence of several peaks around 1000 m high. The central part is dominated by hills and scattered basins. The northeast portion is dominated by an alluvial plain.

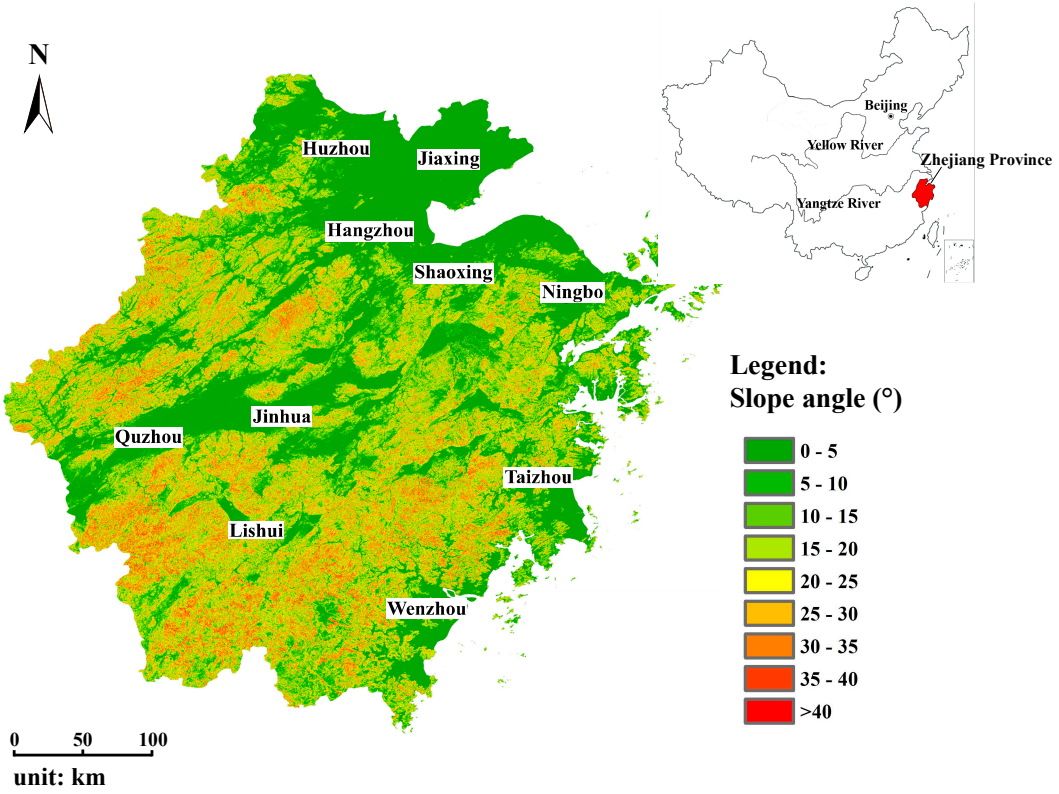

Figure 1. Topographic map of Zhejiang Province generated from 500 × 500 m digital elevation model.

This region suffers from complex geological and extreme climatic settings. Figure 2 shows the exposed bedrock in the mountainous area that consists mainly of intensely weathered granite and tuff [49]. With a geochemical process, the bedrock received strong weathering in this region. The degree of fragmentation alters from intact rock to gravel-like based on the degree of weathering. Generally, these weathering profiles have more complex engineering properties than other sedimentary soils [50]. Located in the coastal region, rainstorms are frequently encountered from May to October. The annual precipitation is around 1380 mm, and the maximum monthly precipitation of over 200 mm is typically recorded in June [51]. The weak geological properties and heavy rainfall brought by typhoon lead to geological disasters of great frequency and scale, which cost significant damages to lives and properties [52]. According to the geological investigation report in the research area from Department of Land and Resources of Zhejiang Province, 2832 geological disasters occurred in the recent five years, resulting in more than 50 civilian casualties as well as a direct economic loss of around US$40 million [53]. Prevention of geohazards is therefore of great importance in Zhejiang province. Similar disaster events have been reported worldwide, showing a strong demand for reliable field survey and instability assessment methods for disaster prevention [54,55].

To study the applicability of the developed method, a representative area in the central north of Zhejiang province was selected, which was located on a fault and was frequently struck by geohazards. A dataset of 20 rock slopes from 12 locations was collected through geologic survey as shown in Figure 3, where the data meet the requirements for the developed method. The study area is divided into two zones by the NE-striking Jiangshan-Shaoxing fault. The northwest area belongs to the Yangtze paraplatform, where the strata are well developed from middle Proterozoic group to Quaternary of the Cenozoic. The magmatic activity is weak, and sedimentary deposits are well exposed. In contrast, the southeast portion belongs to the Southern China fold system, which undergoes strong magmatism, leading to obvious losses of formation. It is covered with igneous rocks and the outcrops are mainly formed by the Mesozoic and Cenozoic continental sedimentary rocks. There are several distinct

geological outcrops in this region, which belong to various geological periods, such as Proterozoic, Paleozoic, Mesozoic, and Cenozoic.

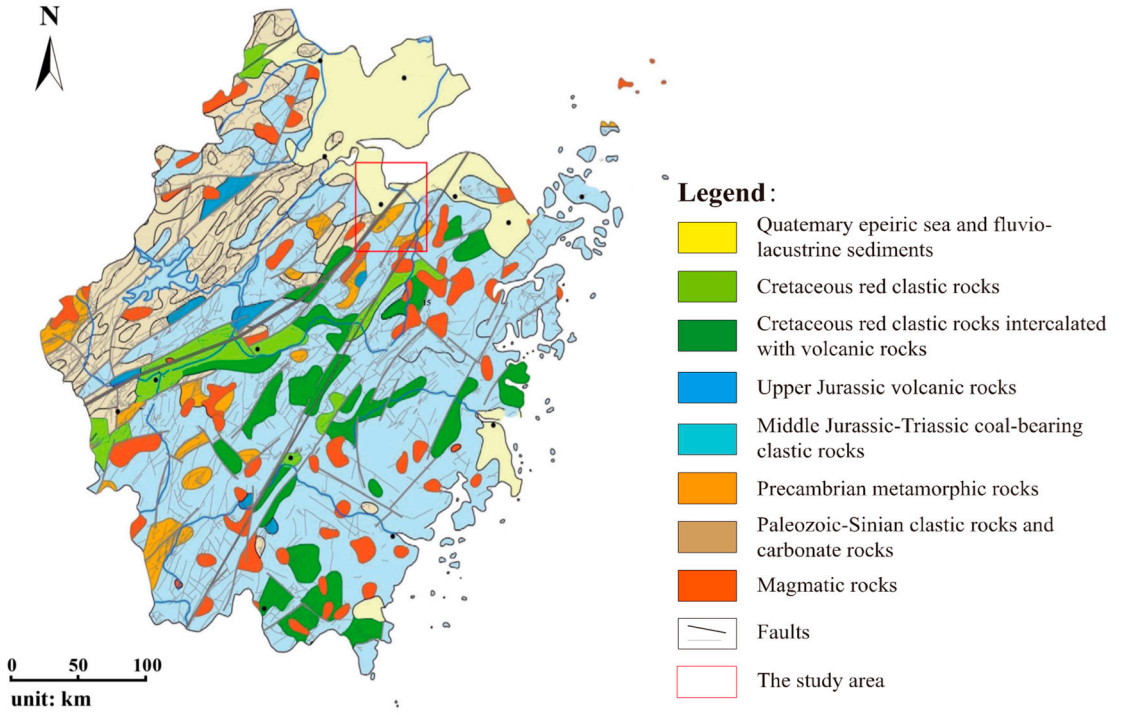

Figure 2. Schematic geological map of Zhejiang Province, China.

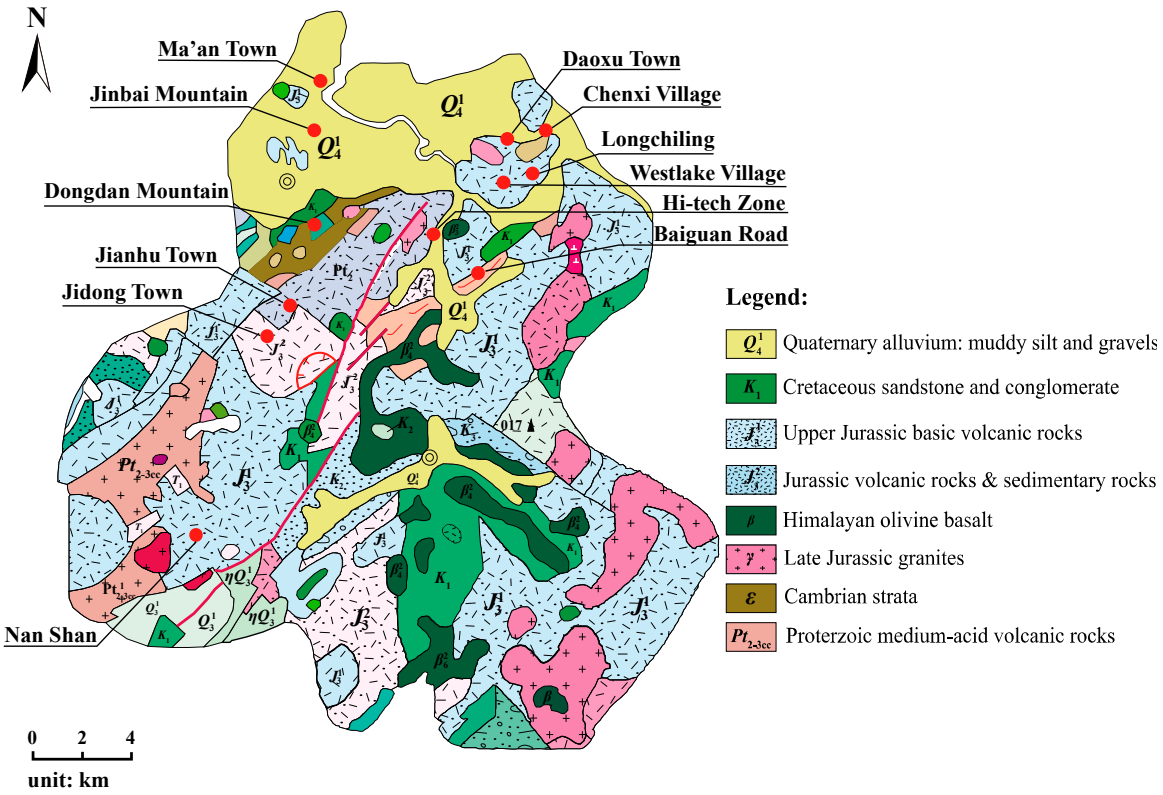

Figure 3. Enlarged view of the geological map of the studied area. (The red points indicate the location of studied slopes.).

3.2. Characteristics of Studied Rock Slopes

A detailed engineering geological survey was conducted on the studied slopes to obtain the main status and characteristics. According to the suggested method by ISRM (2007–2014), point loading test (PL) and Schmidt hammer rebound test (SH) were employed to estimate the characteristics of weathering profiles [56]. Fractured and loose structures dominate the shallow rock masses in the range of 10–20 m combining means of geological logging and drilling data. The dimension of most slopes is small to medium (less than 150 m) and the amount of debris of failed slopes is therefore relatively small. It is indicated from the statistics of geological disasters in the study area that slope failures are bound up with rainfall [49,57,58]. Seismic activities are extremely low, while over half slopes suffered from human activities such as quarrying and road constructions in different degrees. Five of the total 20 slopes have failed in the past, and one example of stable slopes and one example of collapsed slopes are described below to highlight their geological characteristics. Given the close distance, other slopes in the studied area exhibit similar characteristics and the details are quantified by the nine subattributes (Table 1) shown below.

3.2.1. Jidong Town Quarry Slope

Jidong Town rock slope is an abandoned quarry located in the southwest piedmont of Mountain Dabu. It is an excavated slope located in the leading edge of the mountain. The maximum height is 65.8 m, and the slope dip orientation is 265°N. The upper part and the lower part exhibit different geological characteristics as shown in Figure 4. The upper part is covered by debris deposit, including sandy soil mixed with gravels. The measured point loading strength is less than 2 MPa and the rebound number is less than 15, which together with the visual investigation indicate that these rocks are completely weathered. This part has an average height of 18.6 m and an average slope angle of 45°. The lower terrain is steeper (about 85°) than that of the upper part, and the rocks are slightly weathered according to the test results. At the toe of the slope, there is an artificial excavation platform with a width of 54 m. Construction facilities and quarrying induced deposits can be observed on Figure 4.

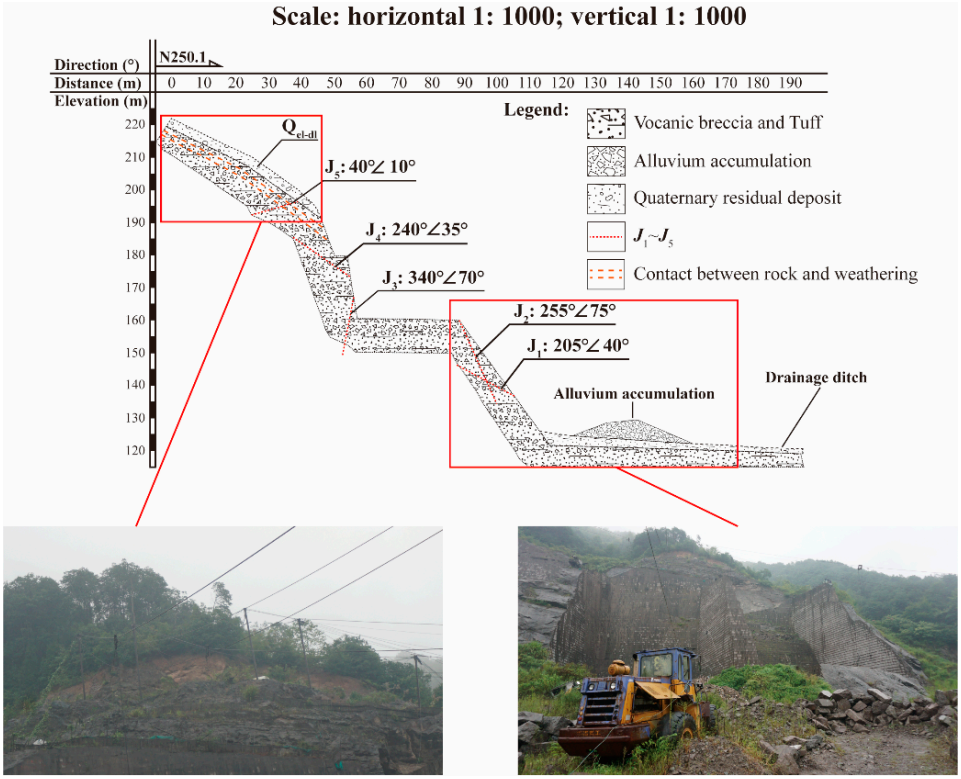

Figure 4. Cross-sectional view and the front views of the Jidong town quarry slope.

Geological logging by fine line method was adopted in the field survey with a total length of 220 m. The results indicated that the slope mainly comprises three joint sets. The orientations of these joints, given as dip direction and dip angle in degrees, are N205∠30–50° (J_1), N340∠65–75° (J_2), and N245∠30–40° (J_3). The spacing of joint sets J_1 and J_2 ranges between 0.5 m and 1 m, while the spacing of joint set J_3 ranges from 1 m to 2 m. The orientation of inclination of the major joint sets is close to that of the slope surface, while their inclination angles are smaller than the slope angle. The tested PL index is over 400 MPa and the SH rebound is over 50 for the bedrock, which indicate that the bedrock has a good quality. Although three sets of joints exist in the slope, they do not form wedges or other structures that are unfavorable to stability. Given these geological features, the Jidong town quarry slope is presently in a stable state, which is also confirmed by the judgment of experts based on in situ survey.

3.2.2. Daoxu Town Quarry Slope

Daoxu Town rock slope is a quarry situated towards the north piedmont of Mountain Chen. The major lithological unit is the lower Cretaceous Gaowu formation. It comprises low-grade ignimbrite in dark grey color and has a loosen structure with lots of cranny. The slope orientation is about N52°∠70° and the average height is 65.8 m. The estimated slope area is about 9000 m^2. As shown in Figure 5, a sudden gradient change appears in the middle of the slope, above which a steep bedrock cliff exists and under which a gentle accumulative zone exists. According to the results of PL and SH tests, the rocks on the top and surfaces are completely decomposed, and the strength is weak.

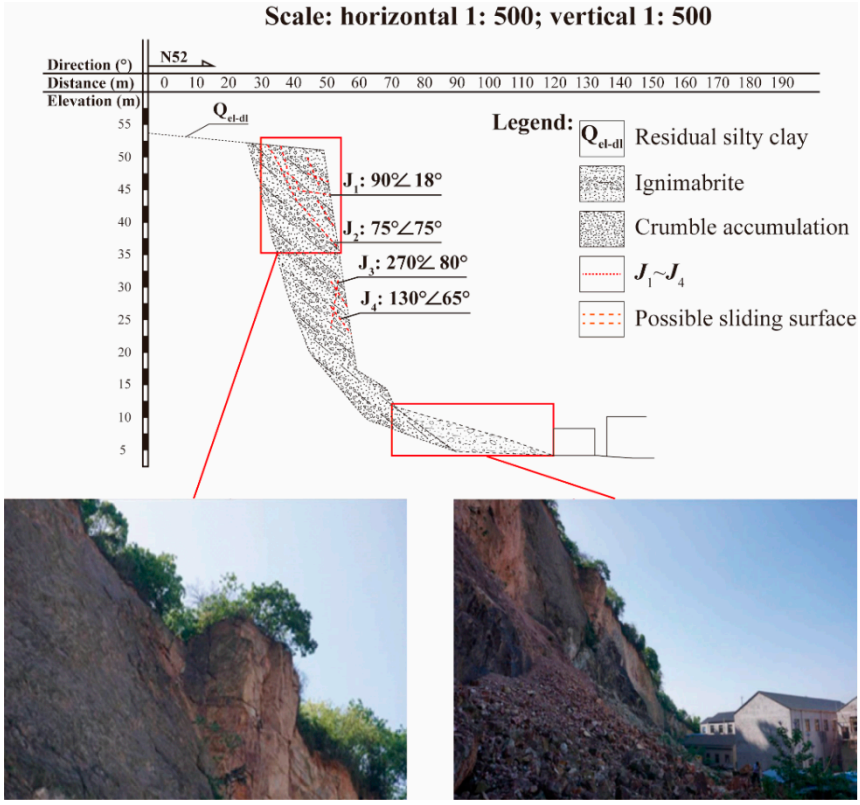

Figure 5. Cross-sectional view and the front views of the Daoxu Town quarry slope.

Four major joint sets were identified and the orientations of them are N90°∠18° (J_1), N75°∠75° (J_2), N270°∠80° (J_3), and N130°∠65° (J_4). Joint sets J_1 and J_2 run parallel to the bedding plane with the spacing varying from 0.5 to 1 m. Because of the large inclination of both joint sets J_3 and J_4, and their spatial correlation with the slope face, wedge-like key blocks hanging on the slope were formed through the combination of these joints (Figure 5). In addition, a great amount of fractures exists in

the slope due to the blasting for quarrying in the past. The hanging rocks of Daoxu Town rock slope collapsed on June 2017 when a monthly precipitation of 208.2 mm and a maximum daily precipitation of 373.4 mm were recorded, and formed the accumulative zone in the toe.

4. Results

Taking Daoxu Town Quarry slope as an example, Tables 4 and 5 tabulate the values for *RMR* and *CSMR* estimations, respectively. A value of 30.8 was obtained by Equations (13) and (14) of the slope, and therefore the slope is classified to grade III, which is in the range from 25 to 50 in *CSMR*. This result revealed the unstable state of the slope, however, given the actual collapsed state, a grade IV should be estimated to fit the reality. It is considered that this discrepancy was yielded due to the incomplete and imprecise information being used in the estimation, which again suggested the necessity of the introduction of probabilistic methods to slope stability assessments.

Table 4. Classification parameters of *RMR* (rock mass rating) for the Daoxu slope.

Category		Value of Parameters	Rating Criteria by Score
Rock strength (MPa)		15–30	3
RQD (rock quality designation) (%)		25–50	8
Spacing of joints		50–100 cm	13
Condition of joints	Roughness	Smooth	1
	Filling	<5 mm (soft)	2
	Aperture	>5 mm	0
	Length	10–20 m	1
	Weathering	Intense weathering	1
Permeability (Lu)		1–10	7
Total		36	

Table 5. Coefficients of correction in the *CSMR* (classification of slope mass rating) estimation.

Category	F_1	F_2	F_3	F_4	λ
Conditions of the slope	10–20	>45°	>120°	Conventional blasting	Jointed rock mass
Coefficients of correction	0.7	1	25	0	0.7

The stability grades for slopes of group A and group B are tabulated in Tables 6 and 7, respectively. These grades were initially determined based on in situ survey data using ordinary estimation methods such as *CSMR*, followed by cross-examination by experienced experts. After modification and validation, these grades mostly represented the actual status of the studied slopes, which are labelled as T_1–T_{10}. Here, Jidong Town quarry slope corresponds to T_4, and Daoxu Town quarry slope corresponds to T_9 in Table 6. There are five slopes that are ranked as IV, which mean that collapse or failure had happened on them.

Table 6. Stability grades for slopes in group A.

H	h	T_1	T_2	T_3	T_4	T_5	T_6	T_7	T_8	T_9	T_{10}
h_1	h_{11}	0.3	0.9	0.4	0.2	0.9	0.1	0.1	0.6	0.9	0.2
	h_{12}	0.8	0.9	0.4	0.1	0.7	0.4	0.1	0.8	0.8	0.9
	h_{13}	0.8	0.9	0.5	0.2	0.7	0.3	0.2	0.8	0.8	0.8
h_2	h_{21}	0.83	0.7	0.42	0.64	0.76	0.83	0.94	0.39	0.81	0.47
	h_{22}	0.07	0.4	0.04	0.21	0.08	0.86	0.67	0.08	0.38	0.15
	h_{23}	0.4	0.6	0.4	0.1	0.6	0.7	0.2	0.3	0.8	0.4
h_3	h_{31}	0.82	0.72	0.7	0.73	0.73	0.7	0.82	0.7	0.8	0.7
	h_{32}	0.8	0.9	0.4	0.2	0.7	0.4	0.2	0.8	0.9	0.8
	h_{33}	0.42	0.42	0.5	0.5	0.42	0.5	0.5	0.5	0.5	0.5
Actual grade		III	IV	II	I	III	II	I	III	IV	III

Table 7. Stability grades for slopes in group B.

H	h	T_1	T_2	T_3	T_4	T_5	T_6	T_7	T_8	T_9	T_{10}
h_1	h_{11}	0.6	0.9	0.4	0.8	0.1	0.4	0.7	0.9	0.1	0.5
	h_{12}	0.7	0.9	0.8	0.6	0.1	0.2	0.9	0.9	0.1	0.5
	h_{13}	0.8	0.9	0.8	0.8	0.2	0.3	0.9	0.8	0.2	0.6
h_2	h_{21}	0.56	0.67	0.89	0.72	0.72	0.81	0.88	0.64	0.72	0.53
	h_{22}	0.13	0.23	0.23	0.1	0.43	0.22	0.16	0.07	0.37	0.4
	h_{23}	0.5	0.5	0.6	0.4	0.2	0.3	0.6	0.7	0.2	0.3
h_3	h_{31}	0.7	0.7	0.82	0.82	0.73	0.7	0.73	0.7	0.82	0.72
	h_{32}	0.6	0.9	0.8	0.8	0.2	0.4	0.9	0.8	0.2	0.4
	h_{33}	0.5	0.5	0.42	0.42	0.5	0.42	0.5	0.5	0.5	0.42
Actual grade		III	IV	III	III	I	II	IV	IV	I	II

Three rock slope samples (T_1, T_2, and T_3) from group A were firstly selected to determine the weight w for the attributes, and w_1, w_2, and w_3 for the subattributes. As shown in Table 1, there are three indices for attribute or subattribute, therefore, the weight vector has a form of $W = (x_1, x_2, x_3)$, where $x_1 + x_2 + x_3 = 1$. A simple algorithm based on MATLAB was developed, which tested different combinations of weight values to identify the suitable vector under that the calculated stability grades of T_1, T_2, and T_3 agree with their actual values (III, IV and II) as tabulated in Table 6.

The calculated weight vectors are as follows.

1. For attributes, $W = (0.6, 0.3, 0.1)$.
2. For subattributes, $W_1 = (0.3, 0.5, 0.2)$, $W_2 = (0.2, 0.2, 0.6)$, and $W_3 = (0.2, 0.4, 0.4)$.

This set of weight vectors was employed to estimate the stability of slopes of group B via Equation (12). Note that in calculation, all the single values tabulated in Table 6 should be expressed as neutrosophic number. For example, a single value 0.3 is transformed into [0.3, 0.3], and its neutrosophic number is $N = 0.3 + 0 \times I$.

The calculated possibilities D_W of each grade for the slopes in group B are tabulated in Table 8. The maximum value of D_W for each slope represents its calculated stability grade. Comparison between the calculated and the actual grades shows that the stability grades of slopes T_2, T_7, and T_8 are underestimated using the current set of weight vector. The accuracy is 70% when the weight vectors are determined based on the data of three slopes.

Table 8. The calculated stability grades for the slopes of group B using weight vectors determined by three samples.

T	D_{W1} (I, T)	D_{W2} (II, T)	D_{W3} (III, T)	D_{W4} (IV, T)	Calculated Grade	Actual Grade
1	0.425	0.875	0.939	0.885	III	III
2	0.357	0.814	0.939	0.928	III	IV
3	0.409	0.852	0.928	0.890	III	III
4	0.435	0.851	0.911	0.865	III	III
5	0.552	0.548	0.476	0.406	I	I
6	0.606	0.804	0.705	0.603	II	II
7	0.374	0.823	0.934	0.921	III	IV
8	0.928	0.926	0.785	0.354	I	IV
9	0.554	0.550	0.474	0.402	I	I
10	0.498	0.901	0.895	0.798	II	II

In the next step, five slope samples (T_1, T_2, T_3, T_4, and T_5) from group A were selected to determine the weight vectors and the results are as follows.

1. For attributes, W = (0.6, 0.2, 0.2);
2. For subattributes, W_1 = (0.3, 0.5, 0.2), W_2 = (0.2, 0.3, 0.5), and W_3 = (0.2, 0.65, 0.15).

The calculated stability categories are tabulated in Tables 9 and 10. In this case, the accuracy increased to 80%, but the stability grades of T_2 and T_7 were still mismatched.

Table 9. The calculated stability grades for the slopes of group B using weight vectors determined by five samples.

T	D_{W1} (I, T)	D_{W2} (II, T)	D_{W3} (III, T)	D_{W4} (IV, T)	Calculated Grade	Actual Grade
1	0.423	0.877	0.943	0.893	III	III
2	0.344	0.804	0.942	0.941	III	IV
3	0.403	0.849	0.931	0.898	III	III
4	0.418	0.846	0.923	0.887	III	III
5	0.559	0.551	0.473	0.401	I	I
6	0.604	0.817	0.717	0.614	II	II
7	0.357	0.809	0.938	0.936	III	IV
8	0.352	0.785	0.926	0.931	IV	IV
9	0.560	0.552	0.470	0.380	I	I
10	0.495	0.910	0.906	0.811	II	II

Table 10. The calculated stability grades for the slopes of group B using weight vectors determined by eight samples.

T	D_{W1} (I, T)	D_{W2} (II, T)	D_{W3} (III, T)	D_{W4} (IV, T)	Calculated Degree	Actual Degree
1	0.420	0.881	0.953	0.904	III	III
2	0.343	0.803	0.947	0.950	IV	IV
3	0.401	0.848	0.938	0.908	III	III
4	0.414	0.851	0.933	0.900	III	III
5	0.569	0.546	0.460	0.389	I	I
6	0.608	0.816	0.717	0.615	II	II
7	0.352	0.810	0.947	0.949	IV	IV
8	0.346	0.792	0.941	0.949	IV	IV
9	0.570	0.546	0.458	0.387	I	I
10	0.503	0.910	0.901	0.807	II	II

Repeating this procedure, it was found that when six samples were used for the determination of weight vectors, the accuracy increased up to 90%. Finally, when eight samples were used for the determination, the accuracy became 100%. The determined weight vectors are

1. For attributes, $W = (0.6, 0.2, 0.2)$;
2. For subattributes, $W_1 = (0.3, 0.5, 0.2)$, $W_2 = (0.2, 0.2, 0.6)$, and $W_3 = (0.2, 0.7, 0.1)$.

5. Discussions

Generally, a greater weight value indicates that an attribute or a subattribute is more intimately correlated with the stability of a slope. The determined weight vector for the three attributes (0.6, 0.2, 0.2) shows that the rock mass characteristics play the most important role in the stability of slopes, which agrees with the common understanding that the physical, mechanical, and geological properties of rock masses govern the stability of rock slopes [4,8,14,17,25,46,47]. Meanwhile, among the three subattributes of the rock mass characteristics, rock structure has greater importance over other two indexes, which is in line with the actual situation that most studied instable slopes are formed by bedding structures with multiple joint sets [59]. Moreover, the plant cover is particularly important in the topographic features, which agrees with the fact that most failed slopes in the studied area are barely covered by plants mainly due to human activities such as quarrying, and road and house constructions as demonstrated by the Daoxu Town quarry slope. Although the precipitation and seismic intensity are almost identical for all the studied slopes given the limited area selected, the precipitation seems to have greater importance than the seismic intensity. In situ survey showed that the majority of failure incidents of studied slopes happened after heavy rainfalls, such as the Daoxu Town quarry slope, demonstrating the important role precipitation plays in the stability of slopes. The maximum daily precipitation may be a better parameter for characterizing the influence of rainfall as long as the data are available. It is noted that the seismic intensity in Zhejiang Province is remarkably low, and no strong earthquakes have been recorded in recent 50 years.

These results show that the rock slopes formed by bedding structures of fractured rocks disturbed by human activities and undergone heavy rainfall are most unstable, which are in concert with our common knowledge on slope stability [60–62]. The developed method can help quantitatively reveal the relative importance of different influencing factors, and help pinpoint the key factors that trigger instability of slopes. This could contribute to the policy-making regarding maintenance works of slopes.

The above results and analysis indicate that the developed method holds a straightforward computational manner. Compared with other probabilistic methods such as ANN that typically require a complex learning process for updating stability knowledge [63,64], the present method only requires a simple trial-and-error approach to determine the weight vector. Meanwhile, ANN requires a large amount of data that possess the main characteristics of a problem for learning and training, which need to be repeated when new data are included in the assessment. In contrast, the requirement of data amount is significantly small by the present method, making it suitable for application to regional slope stability assessment with limited geological survey data. Once an effective weight vector is determined, the method can be applied to the slopes of a whole region possessing similar geological background. Given the simplicity in computation and low demand on input data, this method, supported by expert opinion, can serve as a fast and reliable tool for regional stability assessment of rock slopes.

6. Conclusions

The present study developed a vector similarity measure under neutrosophic number environment for rock slope stability assessments with multiple levels of attributes. The advantage of the method lies on that it significantly simplifies the computational process of fuzzy problems with indeterminate information while maintaining the capability of similarity analysis on multiattribute information based on limited input data.

When applying this method, the weight vector has to be firstly determined based on the data of at least eight slope samples. This amount of data supply is much lower than other representative

probabilistic methods. The determined weight vector reflects the relative importance of different parameters on the stability of slopes in a studied region. It could help understand the key influential parameters for the stability of a slope and take corresponding measures to improve the stability. By incorporating this vector into the multiattribute classification of the influential parameters of slope stability, the developed method can accurately estimate the stability degree of studied slopes. This method does not require sophisticated modeling of slopes and the data demand is relatively low. It could serve as a quick preliminary method to identify the key influential parameters and the risk of rock slope failures. Thorough in situ survey and real-time monitoring could then be applied to the identified slopes at risk to save cost and time.

In the present study, the weight vector was determined via a trial-and-error manner using different amounts of data. In the future, this procedure needs to be improved by developing an algorithm for weight determination. This method will be applied to multiple regions with insufficient or incomplete geological survey data to verify its applicability. The attributes and subattributes need to be continuously improved to establish a more efficient classification system that fits the neutrosophic theory and could well represent the geological characteristics of studied regions.

Author Contributions: Conceptualization, B.L.; Methodology, J.Y.; Software, J.Y.; Validation, B.L., K.Z. and P.S.; Resources, K.Z.; Data Curation, B.L. and P.S.; Writing—Original Draft Preparation, K.Z. and P.S.; Writing—Review & Editing, B.L.; Visualization, P.S.; Supervision, J.Y.; Project Administration, B.L.; Funding Acquisition, B.L. and P.S.

Funding: This research was funded by National Natural Science Foundation of China grant number 51609136 and Zhejiang Provincial Natural Science Foundation of China Grant No. LGF18D020002.

Conflicts of Interest: The authors declare that there are no conflict of interest regarding the publication of this article.

References

1. Einstein, H.H.; Veneziano, D.; Baecher, G.B. The effect of discontinuity Persistence an Rock Slope Stability. *Int. J. Rock Mech. Min. Sci. Geomech. Abstr.* **1983**, *20*, 227–236. [CrossRef]
2. Huang, R.; Fan, X. The landslide story. *Nat. Geosci.* **2013**, *6*, 325–326. [CrossRef]
3. Clayton, A.; Stead, D.; Kinakin, D. Engineering geomorphological interpretation of the Mitchell Creek Landslide, British Columbia, Canada. *Landslides* **2017**, *14*, 1655–1675. [CrossRef]
4. He, M.C.; Tao, Z.G.; Zhang, B. Application of remote monitoring technology in landslides in the Luoshan mining area. *Min. Sci. Technol.* **2009**, *19*, 609–614. [CrossRef]
5. Bishop, A.W. The use of the Slip Circle in the Stability Analysis of Slopes. *Géotechnique* **1955**, *5*, 7–17. [CrossRef]
6. Chen, Z.Y.; Morgenstern, N.R. Extensions to the generalized method of slices for stability analysis. *Can. Geotech. J.* **1983**, *20*, 104–119. [CrossRef]
7. Fellenius, B.H. Static capacity prediction by dynamic methods for three bored piles. *J. Geotech. Geoenviron. Eng.* **2001**, *126*, 640–649. [CrossRef]
8. Kulatilake, P.H.; Wang, L.; Tang, H.; Liang, Y. Evaluation of rock slope stability for Yujian River dam site by kinematic and block theory analyses. *Comput. Geotech.* **2011**, *38*, 846–860. [CrossRef]
9. Ning, Y.J.; An, X.M.; Ma, G.W. Footwall slope stability analysis with the numerical manifold method. *Int. J. Rock Mech. Min. Sci.* **2011**, *48*, 964–975. [CrossRef]
10. Jiang, Q.; Qi, Z.; Wei, W.; Zhou, C. Stability assessment of a high rock slope by strength reduction finite element method. *Bull. Eng. Geol. Environ.* **2015**, *74*, 1153–1162. [CrossRef]
11. Stead, D.; Wolter, A. A critical review of rock slope failure mechanisms: The importance of structural geology. *J. Struct. Geol.* **2015**, *74*, 1–23. [CrossRef]
12. Calista, M.; Miccadei, E.; Pasculli, A.; Piacentini, T.; Sciarra, M.; Sciarra, N. Geomorphological features of the Montebello sul Sangro large landslide (Abruzzo, Central Italy). *J. Maps* **2016**, *12*, 882–891. [CrossRef]
13. Duzgun, H.S.B.; Yucemen, M.S.; Karpuz, C. A probabilistic model for the assessment of uncertainties in the shear strength of rock discontinuities. *Int. J. Rock Mech. Min. Sci.* **2002**, *39*, 743–754. [CrossRef]
14. Stead, D.; Eberhardt, E.; Coggan, J.S. Developments in the characterization of complex rock slope deformation and failure using numerical modelling techniques. *Eng. Geol.* **2006**, *83*, 217–235. [CrossRef]

15. Duzgun, H.B.; Bhasin, R.K. Probabilistic Stability Evaluation of Oppstadhornet Rock Slope, Norway. *Rock Mech. Rock Eng.* **2009**, *42*, 729–749. [CrossRef]
16. Lu, P.; Rosenbaum, M.S. Artificial Neural Networks and Grey Systems for the Prediction of Slope Stability. *Nat. Hazards* **2003**, *30*, 383–398. [CrossRef]
17. Li, W.X.; Mei, S.H. Fuzzy system method for the design of a jointed rock slope. *Int. J. Rock Mech. Min. Sci.* **2004**, *41*, 569–574. [CrossRef]
18. Guo, R.; Zari, M.; Liu, X. Stability evaluation method of rock mass slope based on adaptive neural-network based fuzzy interference system. *Chin. J. Rock Mech. Eng.* **2006**, *25*, 2785–2789. [CrossRef]
19. Melchiorre, C.; Abella, E.C.; Westen, C.V.; Matteucci, M. Evaluation of prediction capability, robustness, and sensitivity in non-linear landslide susceptibility models, Guantánamo, Cuba. *Comput. Geosci.* **2011**, *37*, 410–425. [CrossRef]
20. Park, H.J.; Um, J.G.; Woo, I.; Kim, J.W. Application of fuzzy set theory to evaluate the probability of failure in rock slopes. *Eng. Geol.* **2012**, *125*, 92–101. [CrossRef]
21. Wang, K.; Xu, F. Slope Stability Evaluation Based on PSO-PP. *Appl. Mech. Mater.* **2011**, *580–583*, 486–489. [CrossRef]
22. Li, A.J.; Cassidy, M.J.; Wang, Y.; Merifield, R.S.; Lyamin, A.V. Parametric Monte Carlo studies of rock slopes based on the Hoek–Brown failure criterion. *Comput. Geotech.* **2012**, *45*, 11–18. [CrossRef]
23. Li, W.X.; Qi, D.L.; Zheng, S.F.; Ren, J.C.; Li, J.F.; Yin, X. Fuzzy mathematics model and its numerical method of stability analysis on rock slope of opencast metal mine. *Appl. Math. Model.* **2015**, *39*, 1784–1793. [CrossRef]
24. Park, H.J.; Lee, J.H.; Kim, K.M.; Um, J.G. Assessment of rock slope stability using GIS-based probabilistic kinematic analysis. *Eng. Geol.* **2016**, *203*, 56–69. [CrossRef]
25. Zhao, L.H.; Zuo, S.; Li, L.; Lin, Y.L.; Zhang, Y.B. System reliability analysis of plane slide rock slope using Barton-Bandis failure criterion. *Int. J. Rock Mech. Min. Sci.* **2016**, *88*, 1–11. [CrossRef]
26. Vu-Bac, N.; Lahmer, T.; Zhuang, X.; Nguyen-Thoi, T.; Rabczuk, T. A software framework for probabilistic sensitivity analysis for computationally expensive models. *Adv. Eng. Softw.* **2016**, *100*, 19–31. [CrossRef]
27. Dorren, L.K.A.; Maier, B.; Putters, U.S.; Seijmonsbergen, A.C. Combining field and modelling techniques to assess rockfall dynamics on a protection forest hillslope in the european alps. *Geomorphology* **2004**, *57*, 151–167. [CrossRef]
28. Hess, D.M.; Leshchinsky, B.A.; Bunn, M.; Mason, H.B.; Olsen, M.J. A simplified three-dimensional shallow landslide susceptibility framework considering topography and seismicity. *Landslides* **2017**, *14*, 1677–1697. [CrossRef]
29. Pasculli, A.; Calista, M.; Sciarra, N. Variability of local stress states resulting from the application of Monte Carlo and finite difference methods to the stability study of a selected slope. *Eng. Geol.* **2018**, *245*, 370–389. [CrossRef]
30. Kong, L.; Wu, Y.; Ye, J. Misfire fault diagnosis method of gasoline engines using the cosine similarity measure of neutrosophic numbers. *Neutrosophic Sets Syst.* **2015**, *8*, 42–45. [CrossRef]
31. Chen, J.; Ye, J.; Du, S. Expressions of Rock Joint Roughness Coefficient Using Neutrosophic Interval Statistical Numbers. *Symmetry* **2017**, *9*, 123. [CrossRef]
32. Fu, J.; Ye, J. Simplified neutrosophic exponential similarity measures for the initial evaluation/diagnosis of benign prostatic hyperplasia symptoms. *Symmetry* **2017**, *9*, 154. [CrossRef]
33. Smarandache, F. *Neutrosophy: Neutrosophic Probability, Set, and Logic: Analytic Synthesis & Synthetic Analysis*; American Research Press: Rehoboth, NM, USA, 1998.
34. Smarandache, F. Introduction to Neutrosophic Measure, Neutrosophic Integral, and Neutrosophic Probability. *Comput. Sci.* **2013**, *22d*, 13–25.
35. Smarandache, F. Preface: An introduction to neutrosophy, neutrosophic logic, neutrosophic net, and neutrosophic probability and statistics. In *Proceedings of the First International Conference on Neutrosophy, Neutrosophic Logic, Neutrosophic Set, Neutrosophic Probability and Statistics*; University of New Mexico: Albuquerque, NM, USA, 2002; pp. 5–21.
36. Ye, J. Cosine similarity measures for intuitionistic fuzzy sets and their applications. *Math. Comput. Model.* **2011**, *53*, 91–97. [CrossRef]
37. Ye, J. Multicriteria Group Decision-Making Method Using Vector Similarity Measures for Trapezoidal Intuitionistic Fuzzy Numbers. *Group Decis. Negot.* **2012**, *21*, 519–530. [CrossRef]

38. Ye, J. Bidirectional projection method for multiple attribute group decision making with neutrosophic numbers. *Neural Comput. Appl.* **2015**, *28*, 1021–1029. [CrossRef]
39. Roy, R.; Das, P. A multi-objective production planning problem based on NS linear programming approach. *Int. J. Fuzzy Math. Arch.* **2015**, *8*, 81–91. [CrossRef]
40. Abdel-Basset, M.; Mohamed, M.; Smarandache, F.; Chang, V. Neutrosophic Association Rule Mining Algorithm for Big Data Analysis. *Symmetry* **2018**, *10*, 106. [CrossRef]
41. Ye, J. Multicriteria decision-making method using the Dice similarity measure based on the reduct intuitionistic fuzzy sets of interval-valued intuitionistic fuzzy sets. *Appl. Math. Model.* **2012**, *36*, 4466–4472. [CrossRef]
42. Dice, L.R. Measures of the amount of ecologic association between species. *Ecology* **1945**, *26*, 297–302. [CrossRef]
43. The National Standards Compilation Group of Peoples Republic of China. *GB/T 50330-2013 Technical Code for Building Slope Engineering*; China Planning Press: Beijing, China, 2014.
44. Budetta, P. Assessment of rockfall risk along roads. *Nat. Hazards Earth Syst. Sci.* **2004**, *4*, 71–81. [CrossRef]
45. Romana, M. New Adjustment Ratings for Application of Bieniawski Classification to Slopes. In Proceedings of the International Symposium on the Role of Rock Mechanics; International Society for Rock Mechanics: Salzburg, Austria, 1985; pp. 49–53.
46. Pinheiro, M.; Sanches, S.; Miranda, T.; Neves, A.; Tinoco, J.; Ferreira, A. A new empirical system for rock slope stability analysis in exploitation stage. *Int. J. Rock Mech. Min. Sci.* **2015**, *76*, 182–191. [CrossRef]
47. Qi, C.; Wu, J.; Liu, J.; Kanungo, D.P. Assessment of complex rock slope stability at Xiari, southwestern China. *Bull. Eng. Geol. Environ.* **2016**, *75*, 537–550. [CrossRef]
48. Bieniawski, Z.T. *Engineering Rock Mass Classifications*; Wiley: New York, NY, USA, 1989; pp. 231–243.
49. Ma, T.; Li, C.; Lu, Z.; Bao, Q. Rainfall intensity-duration thresholds for the initiation of landslides in Zhejiang Province, China. *Geomorphology* **2015**, *245*, 193–206. [CrossRef]
50. Lan, H.X.; Hu, R.L.; Yue, Z.Q.; Lee, C.F.; Wang, S.J. Engineering and geological characteristics of granite weathering profiles in South China. *J. Asian Earth Sci.* **2003**, *21*, 353–364. [CrossRef]
51. Ma, T.; Li, C.; Lu, Z.; Wang, B. An effective antecedent precipitation model derived from the power-law relationship between landslide occurrence and rainfall level. *Geomorphology* **2014**, *216*, 187–192. [CrossRef]
52. Zhang, G.R.; Yin, K.L.; Liu, L.L.; Xie, J.M. Warning System for Rain-Induced Landslides Based on Internet in Zhejiang Province, China. *Earth Sci.—J. China Univ. Geosci.* **2005**, *30*, 250–254. [CrossRef]
53. Department of Land and Resources of Zhejiang Province. Prevention and control of geological disasters in Zhejiang Province in 2016. In Proceedings of the Joint Conference on the Prevention and Control of Geological Hazards in Zhejiang, Hangzhou, China, 20 May 2016.
54. Ietto, F.; Perri, F. Flash flood event (October 2010) in the Zinzolo catchment (Calabria, southern Italy). *Rend. Online Soc. Geol. Ital.* **2015**, *35*, 170–173. [CrossRef]
55. Ietto, F.; Perri, F.; Cella, F. Weathering characterization for landslides modeling in granitoid rock masses of the Capo Vaticano promontory (Calabria, Italy). *Landslides* **2018**, *15*, 43–62. [CrossRef]
56. Ulusay, R. *The ISRM Suggested Methods for Rock Characterization, Testing and Monitoring: 2007–2014*; Springer: Basel, Switzerland, 2015.
57. Wei, Z.; Shang, Y.; Zhao, Y.; Pan, P.; Jiang, Y. Rainfall threshold for initiation of channelized debris flows in a small catchment based on in-site measurement. *Eng. Geol.* **2016**, *217*, 23–34. [CrossRef]
58. Gan, J.; Fan, J.; Tang, C.; Wang, C.; Liu, Z.; Li, J. Sucun Landslide in Suichang County of Zejiang Province: Characteristices and Failure Mechanism. *J. Catastrophol.* **2017**, *32*, 73–78. [CrossRef]
59. Kemeny, J. The time-dependent reduction of sliding cohesion due to rock bridges along discontinuities: A fracture mechanics approach. *Rock Mech. Rock Eng.* **2003**, *36*, 27–38. [CrossRef]
60. Tacher, L.; Bonnard, C.; Laloui, L.; Aurèle, P. Modelling the behaviour of a large landslide with respect to hydrogeological and geomechanical parameter heterogeneity. *Landslides* **2005**, *2*, 3–14. [CrossRef]
61. Wu, Y.M.; Lan, H.X.; Gao, X.; Li, L.P.; Yang, Z.H. A simplified physically based coupled rainfall threshold model for triggering landslides. *Eng. Geol.* **2015**, *195*, 63–69. [CrossRef]
62. Ma, J.; Tang, H.; Hu, X.; Antonio, B.; Zhang, M.; Zhu, T.W.; Song, Y.J.; Mutasim, A.M. Identification of causal factors for the Majiagou landslide using modern data mining methods. *Landslides* **2016**, *14*, 311–322. [CrossRef]

63. Shamekhi, E.; Tannant, D.D. Probabilistic assessment of rock slope stability using response surfaces determined from finite element models of geometric realizations. *Comput. Geotech.* **2015**, *69*, 70–81. [CrossRef]
64. Pradhan, A.M.S.; Lee, S.R.; Kim, Y.T. A shallow slide prediction model combining rainfall threshold warnings and shallow slide susceptibility in Busan, Korea. *Landslides* **2018**, *15*, 1145–1153. [CrossRef]